Ion assisted deposition of TiO_2, ZrO_2, and SiO_xN_y optical thin films

H.J. Cho and C.K. Hwangbo
Department of Physics, Inha University, Inchon 402-751, Korea

ABSTRACT

Optical and mechanical characteristics of TiO_2, ZrO_2, and SiO_xN_y thin films prepared by ion assisted deposition(IAD) were investigated. IAD films were bombarded by Ar or nitrogen ion beam from a Kaufman ion source while they were grown in as e-beam evaporator. The result shows that the Ar IAD increases the refractive index and packing density of TiO_2 films close to those of the bulk. For ZrO_2 films the Ar IAD increases the average refractive index, decreases the negative inhomogeneity of refractive index, and reverses to the positive inhomogeneity. The optical properties result from improved packing density and denser outer layer next to air, The Ar-ion bombardment also induces the changes in microstructure of ZrO_2 films, such as the preferred (111) orientation of cubic phase, increase in compressive stress, and reduction of surface roughness. Inhomogeneous refractive index SiO_xN_y films were also prepared by nitrogen IAD and the variable refractive index of SiO_xN_y film was applied to fabricate a rugate filter.

1. INTRODUCTION

Due to the large temperature difference between the material melting temperature and film deposition temperature, optical thin films show columnar microstructure.(1) The columnar microstructure evokes many undesirable effects, such as vacuum-to-air spectral shift, lower packing density, and index inhomogeneity. IAD is one of the enhanced thin film deposition techniques which adds an ion source into the thermal or electron beam evaporation system. Due to the simultaneous energetic ion bombardment of growing thin film, the deposited film shows the improved optical, mechanical, and chemical properties.

TiO_2 and ZrO_2 films are widely used as high refractive index materials in optical thin films. In this study, optical and mechanical properties of Ar IAD thin films were investigated as a function of ion momentum p, which is defined by

$$p = \gamma\sqrt{2m_iE_i}$$

where γ is the arrival rate of ion to that of an evaporated particle, m_i is the mass of the ion, and E_i is energy of ion.(2) Also the nitrogen IAD of SiO_xN_y films was studied as a function of ion energy and oxygen backfill pressure. From the results of refractive index variation, a simple sinusoidal rugate filter was fabricated by controlling the oxygen backfill pressure of nitrogen IAD SiO_xN_y film.

2. EXPERIMENTS

All the films were deposited in a box coater with a cryo pump.(3) The base pressure of the chamber was less than 8×10^{-7} torr. A Kaufman ion source was used for producing bombarding ions and the ion beam current density was measured by a Faraday probe. Film deposition rate was controlled by a quartz crystal thickness monitor and all the admitted gases were carefully regulated by the mass flow controller. Also, the film deposition temperature was carefully maintained by using automatically controlled halogen lamps.

The refractive index and extinction coefficient were determined by envelope method.(4) The packing density was determined from the measurement of vacuum-to-air spectral shift and the void fraction was measured by spectroscopic ellipsometry(SE). Stress of ZrO_2 films were calculated from the lattice spacing variation which was measured by X-ray diffractometer.(5) Also the surface roughness was measured by atomic force microscopy.

3. RESULTS AND DISCUSSION

Refractive index variations of Ar IAD TiO_2 films are presented in Fig. 1. When the bombarded p is larger than 0.3 MeV/c, the refractive index of IAD film is 2.20~2.35. These values are about 0.3 higher than that of conventionally deposited film. It is explained that due to the energetic ion bombardment, the columnar microstructure collapses and the denser films are produced.

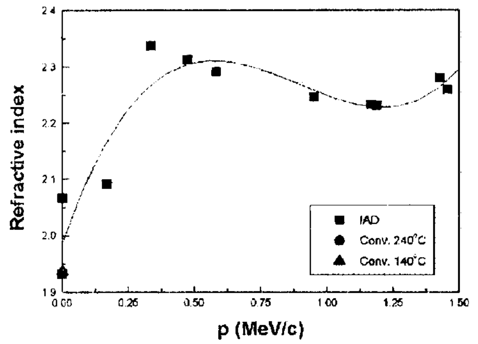

Fig. 1. Refractive index of TiO_2 film as a function of p.

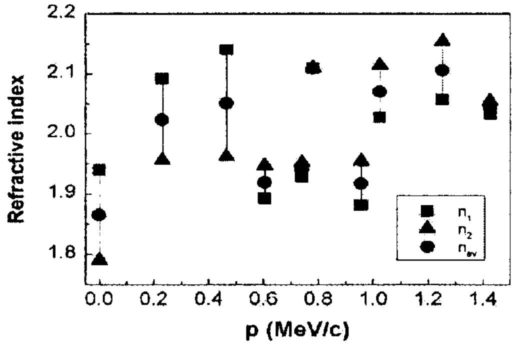

Fig. 2. n_1, n_2, and n_{av} of ZrO_2 films as a function of p.

The inhomogeneous refractive index of IAD ZrO_2 films are determined using an inhomogeneous index model where the refractive index varies linearly with film thickness.(6) From the spectrophotometric measurement of both transmittance and reflectance, we can determine two refractive indices, one is near film-substrate (inner index, n_1) region and the other is the region of film-air (outer index, n_2) side. The average index n_{av} is defined by $(n_1+n_2)/2$. As shown in Fig. 2, the n_{av} increases with p. Conventional and low p IAD films show negative inhomogeneity, which means the n_1 is larger than n_2. However, when p is higher than 0.6 MeV/c, the films have positive

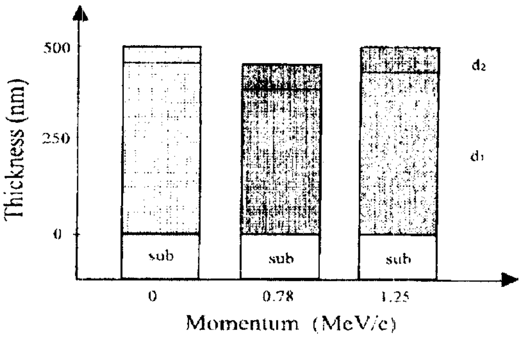

Fig. 3. Variation of void fraction and thickness of the two-layer model ZrO_2 films measured by SE as a function of p.

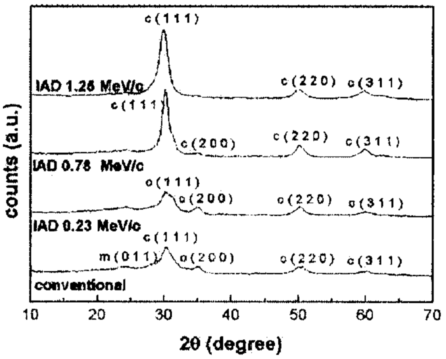

Fig. 4. XRD measurement of ZrO_2 films as a function of p.

inhomogeneity.($n_1<n_2$)

We used spectroscopic ellipsometry to measure the void fraction of the film. A single layer film is modeled as two thin layers. In Fig. 3, the thickness of each layer and void fraction of each layer in gray level are presented. The thickness fraction of bottom layer is about 90 % of total thickness, which means most of ZrO_2 film properties are determined in bottom layer. For p=0 film, the void fraction of top layer is higher than bottom one. This means that the film has negative inhomogeneity. For p=0.78 and p=1.25 films, the void fraction of top layer is smaller than bottom layer. Therefore they have positive inhomogeneity. All of the SE results are consistent with spectrophotometric measurements.

The packing density of TiO_2 and ZrO_2 films are determined from the measurement of vacuum-to-air spectral shift. The results are in Table 1. Conventionally deposited TiO_2 and ZrO_2 films have packing density of 0.65 and 0.81, respectively, while the value of IAD films is 0.97 and 1, respectively. The films produced by IAD have bulk like properties in optical and microstructual aspect. The similar result are obtained for IAD multilayer filters.

Table 1. Vacuum-to-air spectral shift and packing density of TiO_2 and ZrO_2 films.

		refractive index	spectral shift (nm)	packing density
TiO_2 films	conventional	1.94	35.3	0.65
	IAD	2.26	2.7	0.97
ZrO_2 films	conventional	1.86	21	0.81
	IAD	2.11	0	1

The XRD results of ZrO_2 films are shown in Fig. 4. As the p increases, the cubic (111) phase increases preferentially and the monoclinic phase disappears. From these measurements, we can calculate microstrain changes of the films and determine stress of the film. All the films have compressive stress which increases as the p increases. We also measured the surface roughness of

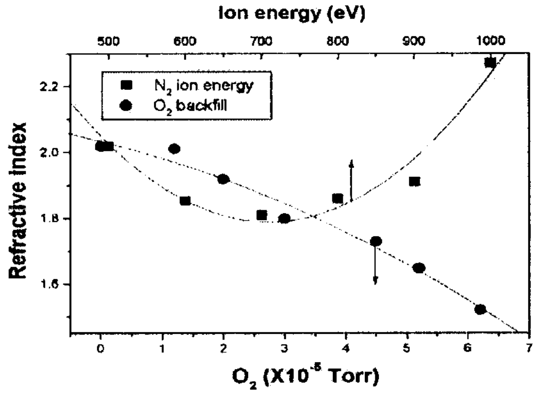

Fig. 5. Refractive index of SiO_xN_y films as a function of oxygen backfill pressure and nitrogen ion energy.

ZrO_2 films using AFM. The rms roughness of the substrate is 6.2Å. The conventional film has 23 Å rms roughness whereas the roughness of IAD films at p=0.23 and p=0.78 MeV/c are 19 and 17 Å, respectively.

SiO_xN_y thin films were fabricated by the nitrogen IAD. The films were produced both by controlling the backfilled oxygen pressure at a constant nitrogen ion energy and by controlling nitrogen ion energy without backfilled oxygen. The refractive index of SiO_xN_y films are determined by envelope method and the results are shown in Fig. 5. The refractive index deposited at zero oxygen backfill pressure is 2.02 of silicon nitride and decreases down to 1.49 of silicon dioxide as the oxygen backfill pressure increases. In nitrogen ion energy variation, the refractive index decreases from 2.02 at 500 eV to 1.82 at 700 eV and then increases up to 2.27 at 1000 eV. However the high energy bombarded film has relatively large extinction coefficient as compare to other films. It seems that the high energy bombarded film was preferentially sputtered by high energy nitrogen ions.

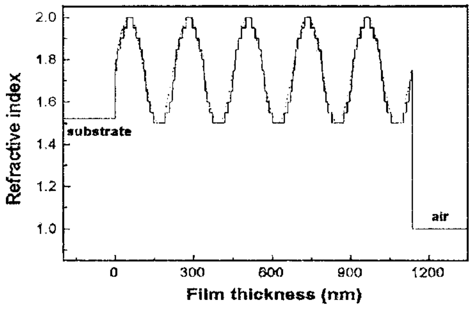

Fig. 6. Refractive index variation of fabricated rugate filter as a function of physical thickness.

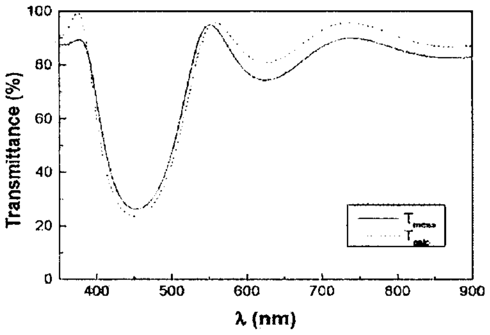

Fig. 7. Transmittance of fabricated and simulated rugate filter.

A simple sinusoidal rugate filter was fabricated by controlling oxygen backfill pressure. Fig. 6 shows the index profile of fabricated rugate filter as a function of film thickness. The continuously varied refractive index was fitted with step index profile with a step of 0.05 and the total thickness of fabricated rugate filter was about 1.2 ㎛.

Spectrophotometric transmittance of a rugate filter with a step index profile is plotted in Fig. 7 and compared with that of simulated one. The transmittance of the fabricated filter is higher than that of calculated one by about 2 % and the FWHM of rejection band is smaller about 5 nm. The difference in transmittance in the short wavelength region is due to the absorption of substrate. Even though there is a little discrepancy between measured and simulated ones, it seems that the refractive index variation by oxygen backfill pressure is well controlled throughout the whole film thickness.

4. CONCLUSIONS

Ar IAD improves optical and microstructual properties of TiO_2 and ZrO_2 films. In ZrO_2 film, the index inhomogeneity reverses from negative to positive as the p increases which is analysed by both spectrophotometric and spectrophotometric ellipsometry. Also the compressive stress and (111) cubic phase increase preferentially as increasing p. The rms surface roughness is improved from 23 Å of conventional film to 17Å by IAD. The refractive index of SiO_xN_y film decreases from 2.02 to 1.49 by varying the oxygen backfilled pressure and the refractive index reaches minimum at 700 eV nitrogen ion energy. A simple sinusoidal rugate filter was fabricated using backfilled oxygen pressure control and the result agrees well with simulated one, except for short wavelength region.

REFERENCES

1. P.J. Martin, R.P. Netterfield, and W.G. Sainty, J. Appl. Phys. **55**, 235 (1983)
2. J.R. McNeil, A.C. Barron, S.R. Wilson and W.C. Herrmann, Jr.,Appl. Opt. **23,** 552 (1984)
3. C.K. Hwangbo, L.J. Lingg, J.P. Lehan, H.A. Macleod, J.L. Makous, and S.Y Kim, Appl. Opt. **28,** 2769 (1989)
4. J.P Lehan, Y. Mao, B.G. Bovard, and H.A. Macleod, Thin Solid Films **203**, 227 (1991)
5. H.J. Cho and C.K. Hwangbo, Appl. Opt. **35**, 5545 (1996)
6. J.C. Manifacier, J. Gasiot, and J.P. Fillard, J. Phys. E **5**, 1002 (1976)
7. H.P. Klug and L.E. Alxander, *X-Ray Diffraction Procedure*, **2** nd Ed. (Wiley, 1974) chap.11 p.757
8. D.P. Arndt, R.M.A. Azzam, J.M. Bennett, J.P. Borgogno, C.K. Carniglia, W.E. Case, J.A. Dobrowolski, U.J. Gibson, T. Tuttle-Hart, F.C. Ho, V.A. Hodgkin, W.P. Klapp, H.A. Macleod, E. Pelletier, M.K. Purvis, D.M. Quinn, D.H. Strome, R. Swenson, P.A. Temple, and T.F. Thonn, Appl. Opt. **23**, 3571 (1984)